

Ipatasertib exhibits anti-tumorigenic effects and enhances sensitivity to paclitaxel in endometrial cancer *in vitro* and *in vivo*

JILLIAN O'DONNELL¹, ZIYI ZHAO^{1,2}, LINDSEY BUCKINGHAM¹, TIANRAN HAO¹, HONGYAN SUO², XIN ZHANG², YALI FAN², CATHERINE JOHN¹, BOER DENG^{1,2}, XIAOCHANG SHEN^{1,2}, WENCHUAN SUN¹, ANGELES ALVAREZ SECORD³, CHUNXIAO ZHOU^{1,4} and VICTORIA L. BAE-JUMP^{1,4}

¹Division of Gynecologic Oncology, University of North Carolina at Chapel Hill, Chapel Hill, NC 27599, USA;

²Department of Gynecologic Oncology, Beijing Obstetrics and Gynecology Hospital, Capital Medical University, Beijing 100006, P.R. China; ³Division of Gynecologic Oncology, Department of Obstetrics and Gynecology, Duke Cancer Institute, Duke University, Durham, NC 27705; ⁴Lineberger Comprehensive Cancer Center, University of North Carolina at Chapel Hill, Chapel Hill, NC 27599, USA

Received March 23, 2023; Accepted June 14, 2023

DOI: 10.3892/ijo.2023.5551

Abstract. Endometrial cancer is the most common gynecologic cancer and one of the only cancers for which incidence and mortality is steadily increasing. Although curable with surgery in the early stages, endometrial cancer presents a significant clinical challenge in the metastatic and recurrent setting with few novel treatment strategies emerging in the past fifty years. Ipatasertib (IPAT) is an orally bioavailable pan-AKT inhibitor, which targets all three AKT isoforms and has demonstrated anti-tumor activity in pre-clinical models, with clinical trials emerging for many cancer types. In the present study, the MTT assay was employed to evaluate the therapeutic efficacy of IPAT or IPAT in combination with paclitaxel (PTX) in endometrial cancer cell lines and primary cultures of endometrial cancer. The effect of IPAT and PTX on the growth of endometrial tumors was evaluated in a transgenic mouse model of endometrial cancer. Apoptosis was assessed using cleaved caspase assays and cellular stress was assessed using ROS, JC1 and tetramethylrhodamine ethyl ester assays. The protein expression levels of markers of apoptosis and cellular stress, and DNA damage were evaluated using western blotting and immunohistochemistry. IPAT

significantly inhibited cell proliferation, caused cell cycle G1 phase arrest, and induced cellular stress and mitochondrial apoptosis in a dose dependent manner in human endometrial cancer cell lines. Combined treatment with low doses of IPAT and PTX led to synergistic inhibition of cell proliferation and induction of cleaved caspase 3 activity in the human endometrial cancer cell lines and the primary cultures. Furthermore, IPAT effectively reduced tumor growth, accompanied by decreased protein expression levels of Ki67 and phosphorylation of S6 in the *Lkb1^{fl/fl}p53^{fl/fl}* mouse model of endometrioid endometrial cancer. The combination of IPAT and PTX resulted in increased expression of phosphorylated-H2AX and KIF14, markers of DNA damage and microtubule dysfunction respectively, as compared with IPAT alone, PTX alone or placebo-treated mice. The results of the present study provide a biological rationale to evaluate IPAT and the combination of IPAT and PTX in future clinical trials for endometrial cancer.

Introduction

It is predicted that in 2023, >66,200 women will be diagnosed with endometrial cancer (EC) and >13,030 women will die of the disease in the United States; this is one of few cancers for which incidence and mortality is steadily increasing, which is thought to be due, at least in part, to the worsening obesity epidemic in the United States (1). Although most endometrial cancer is detected early and is curable with surgery, a substantial proportion of patients are diagnosed with recurrent or metastatic disease (2). Advanced EC has a poor prognosis with a five-year survival of ~17% and median overall survival from time of diagnosis of <12 months (3). Cytotoxic chemotherapy is generally less effective in patients with advanced and recurrent disease and until recently, few other treatment options were available (2,4,5). In fact, prior to the approval of pembrolizumab for the treatment of recurrent or metastatic mismatch repair deficient EC in 2018, no new treatments had been approved by the U.S. Food and Drug Administration for this disease since progestin therapy in the 1970s (4). As

Correspondence to: Professor Victoria L. Bae-Jump, Division of Gynecologic Oncology, University of North Carolina at Chapel Hill, CB 7572, Physicians Office Building Room B105, 170 Manning Drive, Chapel Hill, NC 27599, USA
E-mail: victoria_baejump@med.unc.edu

Dr Chunxiao Zhou, Lineberger Comprehensive Cancer Center, University of North Carolina at Chapel Hill, CB 7295, Lineberger Cancer Center, Room 31-340, 450 West Drive, Chapel Hill, NC 27599, USA
E-mail: czhou@med.unc.edu

Key words: ipatasertib, paclitaxel, synergy, apoptosis, endometrial cancer

tumor genomics has gained traction, better understanding of the molecular drivers of solid tumors has opened the door to the use of newer, targeted therapies in EC (2,6).

A previous genomic analysis reported that the majority of patients with EC have alterations in the PI3K/AKT/mTOR pathway, and this was the case for both endometrioid and serous histologies, as well as for all four EC molecular subtypes in The Cancer Genome Atlas (POLE ultramutated, microsatellite instability hypermutated, copy-number low and copy-number high) (7). Mutations which affect the PI3K/AKT/mTOR pathway cause its activation and allow for unchecked cell proliferation, migration and survival (7). Clinical trials for recurrent or advanced ECs have been previously attempted using mTOR inhibitors both alone and in combination with progestins, selective estrogen receptor modulators and chemotherapy (6,8). Unfortunately, these agents exhibited far lower efficacy than expected, which was thought to be due to lack of target selectivity and the activation of alternative pathways or feedback loops that compensated for the mTOR pathway (6,8). Given this limited success, the use of novel AKT targeting inhibitors, dual inhibitors of AKT and mTOR, or combinations of AKT/mTOR inhibitors with other antineoplastic agents such as DNA repair agents may be an effective treatment strategy for endometrial cancer.

Ipatasertib (IPAT) is an orally administered direct inhibitor of all three isoforms of phosphorylated AKT, upstream from mTOR, and has been reported to show promise in the treatment of certain solid tumors in pre-clinical and clinical trials (9-17). Recent studies have reported that IPAT has anti-proliferative activity and synergy with chemotherapeutic agents in multiple different types of cancer cell lines (7,14,18). *In vivo*, IPAT has been reported to demonstrate efficacy in inhibiting tumor growth alone and in combination with certain chemotherapeutic agents [docetaxel, carboplatin and paclitaxel (PTX)] in mouse models of breast, gastric and prostate cancer (7,14,18). Our previous, recent study demonstrated that IPAT significantly inhibited cell proliferation, induced cell cycle arrest and apoptosis, reduced cellular invasion and increased sensitivity to PTX in uterine serous carcinoma (USC) cells (19).

IPAT has been well-tolerated in phase I and II trials performed in patients including those with breast, lung, gastric and prostate cancer, and is currently under investigation in numerous phase II trials of various solid tumors, including in endometrial cancer combined with megestrol acetate (9,11-13,15-17). IPAT in combination with paclitaxel improved progression-free survival in a phase II trial of triple-negative breast cancer (20). A phase III trial of castrate resistant prostate cancer reported improved progression-free survival (PFS); however, overall survival data is still maturing (21). Given that the PI3K/AKT/mTOR alterations are highly prevalent in endometrioid histology ECs (8), to the present study investigated the anti-tumorigenic properties of IPAT and its synergistic anti-proliferative effect with PTX in human endometrioid EC cell lines, primary cultures of endometrioid EC and a genetically engineered mouse model of endometrioid EC.

Materials and methods

Cell culture and reagents. The EC, HEC-1A and ECC-1 cell lines, were used in the present study. HEC-1A cells were

maintained in McCoy's 5A medium with 10% fetal bovine serum (FBS; Thermo Fisher Scientific, Inc.). ECC-1 cells were cultured in 1640 medium with 5% FBS. Both cell lines were authenticated annually by Labcorp using short tandem repeat profiling. Mycoplasma detection kit (Thermo Fisher Scientific, Inc.) was used to test both cell lines for mycoplasma every six months. All media were supplemented with 100 U/ml of penicillin and 100 ug/ml of streptomycin. The cells were cultured in a humidified 5% CO₂ environment at 37°C. IPAT was donated from Genentech, Inc. PTX was purchased from MedChemExpress. All antibodies were purchased from Cell Signaling Technology, Inc. and ABclonal Biotech Co., Ltd. MTT, crystal violet, DMSO and propidium iodide were purchased from MilliporeSigma.

MTT assay. HEC-1A and ECC-1 cells were plated in 96-well plates at a concentration of 3x10³ and 5x10⁵ cells/well, respectively, and cultured at 37°C for 24 h. The cells were then treated with a range of concentrations of IPAT and PTX for 72 h. MTT (5 mg/ml) was added at a dose of 5 µl/well at the end of treatment. After 1 h of incubation, the MTT reaction was terminated through the addition of DMSO at 100 µl/well. The results were calculated by measuring absorption at 575 nm using a microplate reader (Tecan Group, Ltd.). The effect of IPAT was calculated as a percentage of control cell growth obtained from DMSO-treated cells grown in the same 96-well plates. IC₅₀ values were calculated using an IC₅₀ Calculator (AAT Bioquest, Inc.). Each experiment was performed in triplicate to assess the consistency of the results.

Colony formation assay. HEC-1A and ECC-1 cells were seeded (1,000 cells/well) in 6 cm culture dishes and cultured overnight, and medium was then replaced with fresh growth medium containing the indicated concentrations of IPAT for 72 h. Cells were cultured at 37°C for 14 days with medium changes every three to four days. Cells were stained with 0.5% crystal violet and colonies were counted under the microscope.

Cleaved Caspase 3, 8 and assays. HEC-1A and ECC-1 cells were plated in 6-well plates at a concentration of 3.5x10⁵ and 5x10⁵ cells/well, respectively. After treating with different doses of IPAT and in combination with PTX for 14 h, 150-180 µl of 1x caspase lysis buffer was added into each well. The BCA assay (Thermo Fisher Scientific, Inc.) was used to determine the concentration of protein. Lysates (10-15 ug) in black clear bottom 96-well plates were incubated with reaction buffer and 200 µM of caspase 3, caspase 8 or caspase 9 substrate (AAT Bioquest, Inc.) for 30 min. The fluorescence intensity for cleaved caspase 3 (excitation, 400 nm; emission, 505 nm), cleaved caspase 8 (excitation, 376 nm; emission, 482 nm) and cleaved caspase 9 (excitation, 341 nm; emission 441 nm) was assessed using a Tecan microplate reader. Assays were performed in triplicate and repeated three times.

Cell cycle assay. For cell cycle analysis, HEC-1A and ECC-1 cells were treated with different concentrations of IPAT for 36 h. The cells were harvested using 0.25% trypsin at 37°C and then fixed in 90% ice-cold methanol solution in a cold room for 1 h. The cells were resuspended in RNase A solution for 30 min, followed by staining with propidium iodide

for 10 min at room temperature. All samples were assessed using a Cellometer (Nexcelom Bioscience LLC) to identify cell cycle progression. The results were analyzed using FCS4 express software (Molecular Devices LLC).

Reactive oxygen species (ROS) assay. HEC-1A and ECC-1 cells were plated and grown in 96-well plates at a concentration of 8×10^3 cells/well for 24 h. The cells were then treated with a range of doses of IPAT for an additional 16 h. To measure intracellular ROS production, cells were exposed to the oxidation sensitive probe 2',7'-dichlorofluorescein diacetate (DCFH-DA) at $10 \mu\text{M}$ for 1 h at room temperature. Fluorescence was then quantified at 575 nm using a microplate reader (Tecan Group, Ltd.) and normalized to corresponding MTT measurements of the same plate.

Mitochondrial membrane potential assays. Mitochondrial membrane potential was analyzed using the specific fluorescent probes JC-1 and tetramethylrhodamine ethyl ester (TMRE; AAT Bioquest, Inc.). HEC-1A and ECC-1 cells were plated in 96-well plates at the concentration of 4×10^3 cells/well for the TMRE assay and 1×10^4 cells/well for the JC-1 assay. After 24 h, cells were exposed to a range of doses of IPAT for 16 h. JC-1 ($2 \mu\text{M}$) or TMRE ($80 \mu\text{M}$) were added into each well for 30 min at 37°C . The fluorescence intensity was measured for JC-1 (excitation, 480 nm; emission 590 nm) and TMRE (excitation, 549 nm; emission 575 nm). Each assay was repeated at least three times.

Western blotting. HEC-1A and ECC-1 cells were plated in 6-well plates at a concentration of 5×10^4 cells/well and cultured for 24 h or until 70-80% confluence as assessed using an inverted light microscope. Cells were then treated with different concentrations of IPAT at 37°C for different times, as determined for each experiment. Cell lysates were prepared using RIPA buffer (MilliporeSigma) and isolated protein solutions were maintained on ice. The BCA assay was used to determine the protein concentration. Equal amounts of protein ($30 \mu\text{g}$ /well) were separated by 12% gel electrophoresis and transferred onto a polyvinylidene difluoride (PVDF) membrane. The membranes were blocked using a 5% nonfat milk solution for 1 h at room temperature and then incubated with different primary antibodies overnight at 4°C . All antibodies were from Cell Signaling Technology, Inc. and diluted 1:1,000 against phosphorylated (p)-AKT (cat. no. 9271), p-S6 (cat. no. 4858), CDK4 (cat. no. 12790), CDK6 (cat. no. 3136), Cyclin D1 (cat. no. 2978), Bcl-2 (cat. no. 4223), myeloid cell leukemia-1 (Mcl-1; cat. no. 5453), Bip (cat. no. 3177), PRKR-like endoplasmic reticulum kinase (PERK; cat. no. 5683), Calnexin (cat. no. 2679), protein disulfide isomerase (PDI; cat. no. 3501) and Bcl-xL (cat. no. 2764). The antibodies against α -tubulin (cat. no. 3873) were diluted 1:3,000. Membranes were then washed with TBST solution with 0.1% Tween 20 and incubated with a secondary peroxidase-conjugated antibody for 1 h. Antibody levels were assessed using an enhanced chemiluminescence detection system on the ChemiDoc System (Bio-Rad Laboratories, Inc.). After developing for p-AKT or p-S6, the membranes were stripped and re-probed using pan-AKT (1:1,000; cat. no. 4685) and pan-S6 (1:1,000; cat. no. 2217) antibodies overnight at 4°C , and then incubated

with peroxidase-conjugated goat anti-rabbit secondary antibodies (1:4,000; cat. no. 7074) for 1 h at room temperature. Intensity for each band was measured and normalized to either β -actin or α -tubulin as an internal control. Experiments were performed in triplicate.

Lkb1^{fl/fl}p53^{fl/fl} transgenic mouse model of EC. A *Lkb1^{fl/fl}p53^{fl/fl}* genetically engineered mouse model of EC created previously by our laboratory, has been previously reported for the study of the effects of metabolism and targeted therapy on EC tumor growth (22-24). All mice were handled according to protocols approved by University of North Carolina at Chapel Hill (UNC-CH) Institutional Animal Care and Use Committee (approval no. 20-219). In the UNC animal facility, the mice were housed with a 12 h light/dark cycle at $22 \pm 2^\circ\text{C}$ and were given free access to food and water. At six to eight weeks of age, *Lkb1^{fl/fl}p53^{fl/fl}* mice were injected with one-sided intra-uterine Adenovirus Cre (AdCre, University of Iowa Transfer Vector Core; titer of 10^{11} - 10^{12}) to induce EC in the UNC animal facility. Mice were anesthetized using intraperitoneal injection of 75 mg/kg ketamine and 1 mg/kg medetomidine. Immediately after surgery, mice were injected intraperitoneally with antisedan (1 mg/kg) and buprenorphine (0.1 mg/kg) subcutaneously. Buprenorphine (0.1 mg/kg) was administered subcutaneously to the mice every 8 h for two consecutive days as an analgesic. Eight weeks after tumor induction, the mice were divided into four groups and treated with either IPAT (50 mg/kg, oral gavage, daily), PTX (10 mg/kg, intraperitoneal, weekly), a combination of IPAT (50 mg/kg, oral gavage, daily) with PTX (10 mg/kg, intraperitoneal, weekly), or placebo for 4 weeks. Each group included 25-30 mice. The animals were weighed weekly throughout the study. After 4 weeks of treatment, all mice were anaesthetized using carbon dioxide inhalation (45% volume displacement/min) and once fully anesthetized, euthanized by cervical. The endometrial tumors were then collected, measured and weighed. No tumor >1.5 cm in diameter or 2 g in weight were found. Half of the endometrial tumor was snap-frozen and stored at -80°C , and the other half was fixed in 10% neutral-buffered formalin for 24-48 h at room temperature and paraffin embedded.

Immunohistochemistry (IHC). After the mouse endometrial tumor tissues were formalin-fixed for 24-48 h at room temperature. The tumor tissues were paraffin-embedded at the Animal Histopathology Core Facility at UNC-CH. Slides (tissue thickness, $5 \mu\text{m}$) were first incubated with protein block solution (Dako; Aglient Technologies, Inc.) for 1 h at room temperature and then with the primary antibodies against Ki-67 (1:400; cat. no. 34330; Cell Signaling Technologies, Inc.), p-S6 (1:500; cat. no. 4858; Cell Signaling Technologies, Inc.), p-H2AX (1:100; cat. no. AP0687; ABclonal Biotech Co., Ltd.) and KIF14 (1:150; cat. no. A10275; ABclonal Biotech Co., Ltd.) for 2 h at 37°C . The slides were then washed with TBST with 0.1% Tween 20 and incubated with a biotinylated goat anti-rabbit secondary antibodies (1:250; cat. no. NC9256157, Vector Laboratories, Inc.) at room temperature for 1 h. Further processing was performed using ABC-Staining Kits (Vector Laboratories, Inc.) for 10-15 min at room temperature, and hematoxylin was used for counterstain for 1 min at room temperature. IHC slides were scanned using a Motic EasyScan

instrument (Motic Instruments) and scored using ImagePro software (version 2.1.8; Media Cybernetics, Inc.).

Primary cell cultures of EC. Fourteen tumor specimens were collected from EC patients undergoing hysterectomy at N.C. Women's Hospital. All patients provided written informed consent and approval was obtained from the UNC Institutional Review Board committee (approval no. 20-3013). Tissues were gently washed with PBS and then minced using scissors in DMEM/F12 medium (Gibco; Thermo Fisher Scientific, Inc.). Tissues cells were digested in 0.1% collagenase IA solution (MilliporeSigma) containing 100 U/ml penicillin and streptomycin for 0.5 to 1 h at 37°C. The cells were plated in 96-well plates at 8×10^5 cells/well and 6-well plates at 5×10^4 cells/well, and treated with IPAT or PTX for different time periods at 37°C. Cell proliferation was assessed by MTT assay after 72 h of treatment and western blotting and cleaved caspase 3 assays were performed after 24 h of treatment, all according to the aforementioned methods.

Statistical analysis. All measurement data were presented as mean \pm standard deviation. The differences between two groups were analyzed using an unpaired Student's t-test. Statistical comparison of multiple groups was performed using one-way ANOVA with Tukey's multiple comparison test. Linear regression analysis was performed to analyze the relationship between the expression levels of AKT and S6 phosphorylation and the sensitivity of EC cells to IPAT. Statistical analysis was performed using both SAS (version 9.4; SAS Institute Inc.) and GraphPad Prism (version 8; GraphPad Software; Dotmatics) statistical software packages. All tests were two-sided with $P < 0.05$ considered to indicate a statistically significant difference.

Results

Effect of IPAT on cell proliferation in EC cells. The HEC-1A and ECC-1 EC cell lines were treated with IPAT at different concentrations for 72 h. Cell proliferation was assessed using the MTT assay. IPAT demonstrated a dose dependent reduction in cell proliferation in both cell lines. The IC_{50} dose was 4.65 μ M in HEC-1A and 2.92 μ M in ECC-1 cells, respectively (Fig. 1A). Colony formation assays were performed to evaluate the long-term effects of IPAT on cell growth in these two cell lines. HEC-1A and ECC-1 cells were treated with 0.1, 1 and 10 μ M IPAT for 48 h and then the culture media was changed every 3 days until day 14 of incubation. Colony formation was significantly inhibited at 10 μ M IPAT, in both cell lines. The colony-forming ability of HEC-1A and ECC-1 was reduced by 76.34 and 79.92% respectively, after exposure to 10 μ M of IPAT for 48 h (Fig. 1B). These results suggested that IPAT has a potent anti-proliferative activity in EC cells.

The effect of IPAT on the AKT/mTOR signaling pathway was evaluated using western blotting analysis in the HEC-1A and ECC-1 cell lines. The results demonstrated that treatment with 5 μ M IPAT for 30 min markedly increased the expression of phosphorylated AKT and markedly decreased the expression of phosphorylated S6 in both cell lines. Furthermore, these changes were maintained in a time-dependent manner after increasing the duration of exposure to at least 30 h

(Fig. 1C). Increasing IPAT concentrations increased the expression of phosphorylated AKT (ser473) in HEC-1A cells and decreased phosphorylated expression of S6 (ser235/236) in both cell lines after 24 h of treatment (Fig. 1D). Together, these results demonstrated that IPAT inhibits cell proliferation via the AKT/mTOR/S6 signaling pathway in EC cells.

Effect of IPAT on cell cycle progression in EC cells. To evaluate the effect of IPAT on cell cycle in both cell lines, the cell cycle profile was analyzed after treating the HEC-1A and ECC-1 cells with a range of doses (0.1-10 μ M) of IPAT for 36 h. IPAT induced marked G1 phase arrest with an accompanying decrease in the number of cells in S phase in a dose-dependent fashion in both cell lines. Treatment of HEC-1A and ECC-1 cells with 10 μ M IPAT markedly increased the G1 phase, by 17.81 and 19.4% respectively, and decreased the S phase by 12.28 and 22.16%, respectively (Fig. 2A). Western blotting demonstrated that IPAT markedly downregulated the protein expression levels of cell cycle associated proteins cyclin D1, CDK-4 and CDK-6 with increased doses of IPAT in both cell lines after 24 h of treatment (Fig. 2B).

Effect of IPAT on apoptosis in EC cells. To evaluate whether growth inhibition by IPAT was related to apoptosis, its apoptotic effect on HEC-1A and ECC-1 cells was evaluated using cleaved caspase 3, 8 and 9 assays. HEC-1A and ECC-1 cells were treated with varying concentrations of IPAT for 18 h and a significant dose-dependent increase in the activities of cleaved caspase-3, 8 and 9 was demonstrated when compared with controls (Fig. 3A-C). Treatment of ECC-1 cells with 10 μ M IPAT significantly increased the activities of cleaved caspase-3, cleaved caspase-8 and cleaved caspase-9 by 98.9, 61.8 and 89.8%, respectively. In the HEC-1A cells, 10 μ M IPAT increased the activities of cleaved caspase 3 by 87.6%, cleaved caspase 8 by 53.5% and cleaved caspase 9 by 69.4%, respectively. Furthermore, western blotting for the apoptosis-associated proteins Bcl-2 and Mcl-1 demonstrated a marked dose-dependent decrease with increasing doses of IPAT after 24 h of treatment (Fig. 3D). These results suggested that the inhibition of cell growth and the induction of apoptosis by IPAT depend on both extrinsic and intrinsic apoptotic pathways in EC cells.

Effect of IPAT on cellular stress in EC cells. ROS have been implicated in cellular responses to stress and are involved in the mediation of apoptosis via mitochondrial DNA damage (25). To evaluate the involvement of oxidative stress in the anti-proliferative effect of IPAT in EC cells, intracellular ROS levels were assessed using the ROS fluorescence indicator DCHF-DA. Treatment with different doses of IPAT for 16 h significantly increased cellular ROS production in a dose-dependent fashion in the HEC-1A and ECC-1 cells (Fig. 4A). At a dose of 10 μ M, IPAT significantly increased ROS production by 21.1 and 23.4% in HEC-1A and ECC-1 cells compared with control cells, respectively. Changes in markers for mitochondrial membrane potential were assessed after 16 h of IPAT treatment in both cell lines. Both TMRE and JC-1 assays demonstrated that IPAT reduced mitochondrial membrane potential with increasing doses of IPAT in both cell lines. IPAT (10 μ M) decreased JC1 production by 31.5% and

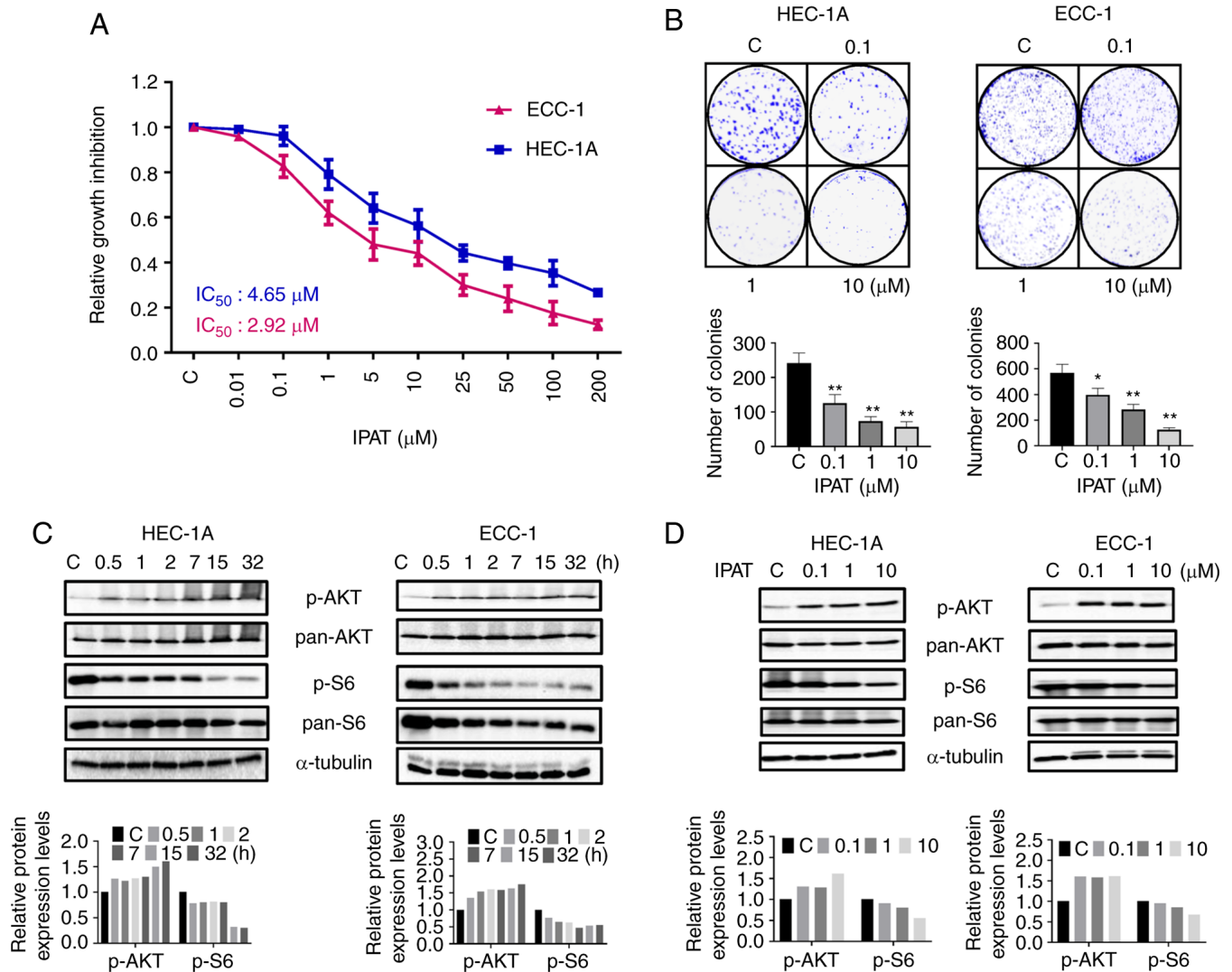


Figure 1. Effect of IPAT on cell proliferation and the AKT/mTOR signaling pathway in endometrial cancer cells. HEC-1A and ECC-1 cells were treated with a range of concentrations of IPAT for 72 h. (A) MTT results demonstrated that IPAT inhibited cell proliferation in a dose-dependent manner in both cell lines. (B) IPAT reduced colony formation in both cell lines. (C) Treatment of both cell lines with 5 μ M IPAT for 30 min enhanced the protein expression levels of p-AKT and decreased those of p-S6, and these effects of IPAT persisted for at least 30 h. (D) Different concentrations of IPAT effectively increased phosphorylation of AKT and downregulated phosphorylation of S6 in both cell lines. * P <0.05 and ** P <0.01. IPAT, ipatasertib; p, phosphorylated; C, control.

TMRE production by 21.1% in HEC-1A cells and decreased JC1 production by 38.1% and TMRE production by 12.5% in ECC-1 cells (Fig. 4B and C). Western blotting demonstrated that IPAT induced the expression of PDI, Calnexin, BiP and PERK which are all cellular stress associated proteins (Fig. 4D). These results suggested that an increase in cellular stress may be one mechanism by which IPAT inhibits cellular proliferation in EC cells.

IPAT demonstrated synergistic activity with paclitaxel in EC cells. As the combination of IPAT and PTX was previously reported to synergistically reduce cell proliferation compared to either agent alone in uterine serous carcinoma cells (19), the present study evaluated whether IPAT could increase the sensitivity of EC cell lines to PTX. PTX effectively inhibited cell proliferation in a dose dependent manner in both cell lines after 72 h of treatment, with an IC₅₀ of 2.93 nM in HEC-1A and 1.13 nM in ECC-1 cells (Fig. 5A). Depending on the effect of IPAT or PTX on cell proliferation, both cell lines were

treated with three different doses of IPAT alone, PTX alone or the combination for 72 h. MTT results demonstrated that the combination of low dose IPAT with PTX produced synergistic activity (combination index <1) compared with monotherapy alone in both cell lines (Fig. 5B). Apoptosis in the cell lines was then assessed, in the presence of either agent alone or in combination, using the ELISA cleaved caspase-3 assay. HEC-1A and ECC-1 cells were treated with IPAT, PTX and the combination of IPAT and PTX for 16 h. Cleaved caspase-3 activity was significantly increased in the combination treatment compared with either agent alone (Fig. 5C). IPAT (1 μ M) increased caspase-3 activity by 84.4 and 43.6%, and 1 nM PTX enhanced caspase-3 activity by 114 and 71.2% in the ECC-1 and HEC-1A cells, respectively. The combination of 1 μ M IPAT and 1 nM PTX was demonstrated to be more potent than each either agent alone in inducing cleaved caspase-3 activity, with a significant 178.2 and 96.6% increase in ECC-1 and HEC-1A cells, respectively. Furthermore, results from the western blotting assay demonstrated that the combination 1 μ M IPAT and

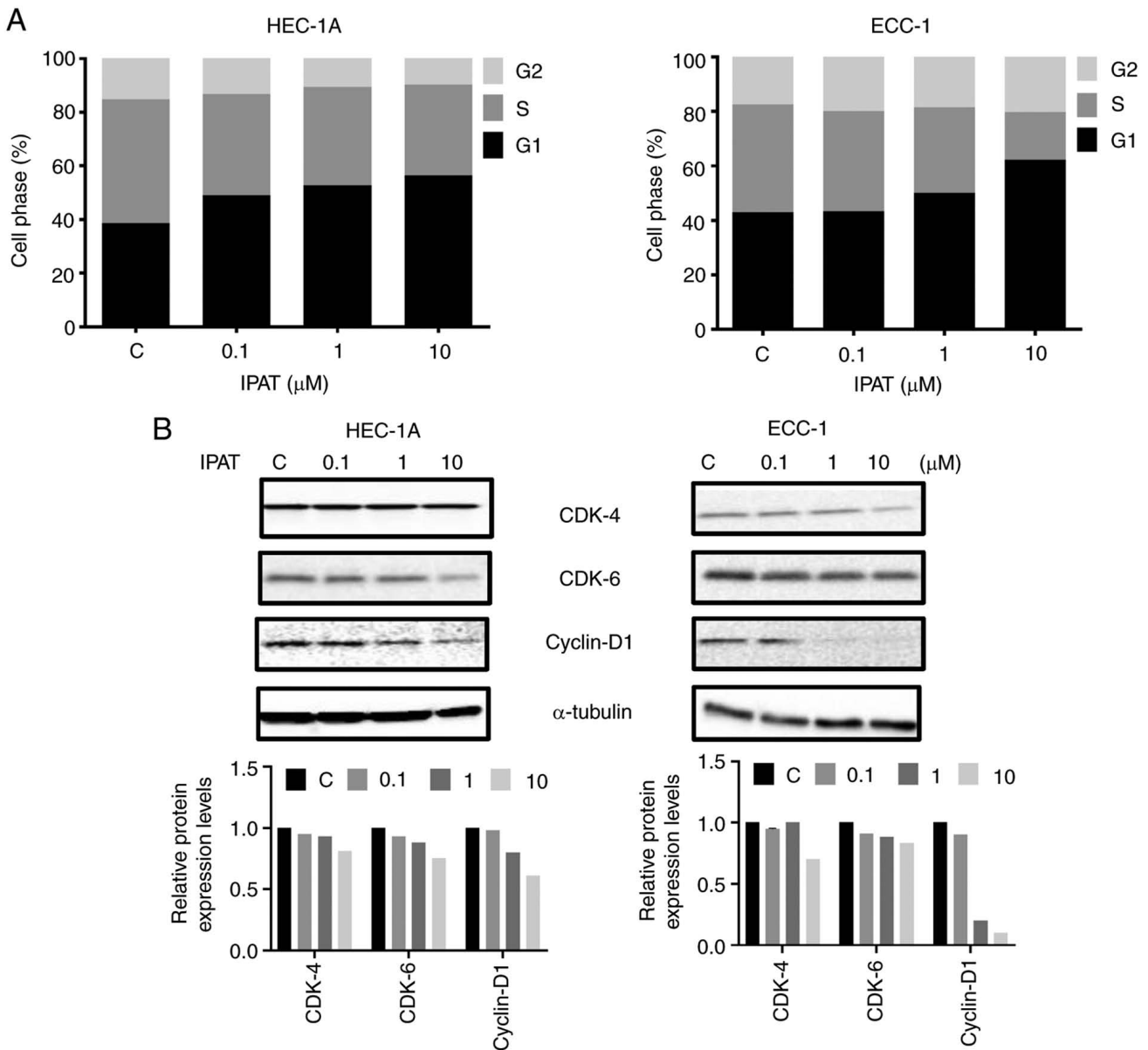


Figure 2. IPAT induced cell cycle G1 arrest in endometrial cancer cells. The HEC-1AA and ECC-1 cells were incubated in the presence of different doses of IPAT for 36 h. (A) IPAT induced dose-dependent cell cycle G1 phase arrest in both cell lines. (B) Western blotting demonstrated a decreasing trend in the protein expression levels of cell-cycle related proteins, including CDK4, CDK6 and cyclinD1 in both cell lines after 24 h of treatment in both cell lines. IPAT, ipatasertib; C, control.

1 nM PTX had a greater ability to reduce the expression of Bcl-xL in HEC-1A and ECC-1 cells compared with control, PTX or IPAT alone (Fig. 5D). These results indicated that the synergistic effect of the combination treatment was due in part to effects on apoptotic pathways in EC cells.

IPAT inhibited tumor growth and increased sensitivity to PTX in vivo. Given that IPAT significantly inhibited EC cell proliferation and induced apoptosis *in vitro*, the effect of IPAT, PTX and the combination of IPAT and PTX on tumor growth in the *Lkb1^{fl/fl}p53^{fl/fl}* mouse model of EC was evaluated. The mice were divided into four groups (25-30 mice per group) and treated with IPAT (50 mg/kg, oral gavage, daily), PTX (10 mg/kg, intraperitoneal, weekly), the combination of IPAT and PTX, or vehicle for 4 weeks, starting 10 weeks after tumor induction with AdCre. During treatment, the daily oral dose

of IPAT was well tolerated without significant toxicity or body weight changes compared with control mice (data not shown). Tumor weights were significantly reduced by 52.2% in the IPAT group compared placebo after 4 weeks of treatment. PTX demonstrated similar anti-tumor activity compared with IPAT, and the combination of IPAT and PTX effectively inhibited tumor growth and exhibited significantly increased anti-tumor efficacy compared with IPAT alone or PTX alone (Fig. 6A).

To explore the mechanism of action underlying synergistic anti-tumor effects of IPAT in combination with PTX, the expression of Ki67, p-S6, p-H2AX and KIF-14 in the endometrial cancer tissues from *Lkb1^{fl/fl}p53^{fl/fl}* mouse model was assessed using immunohistochemistry. IPAT treatment significantly inhibited the expression of p-S6, and the protein expression level of Ki67 was significantly reduced in IPAT, PTX and the combination groups compared with the control

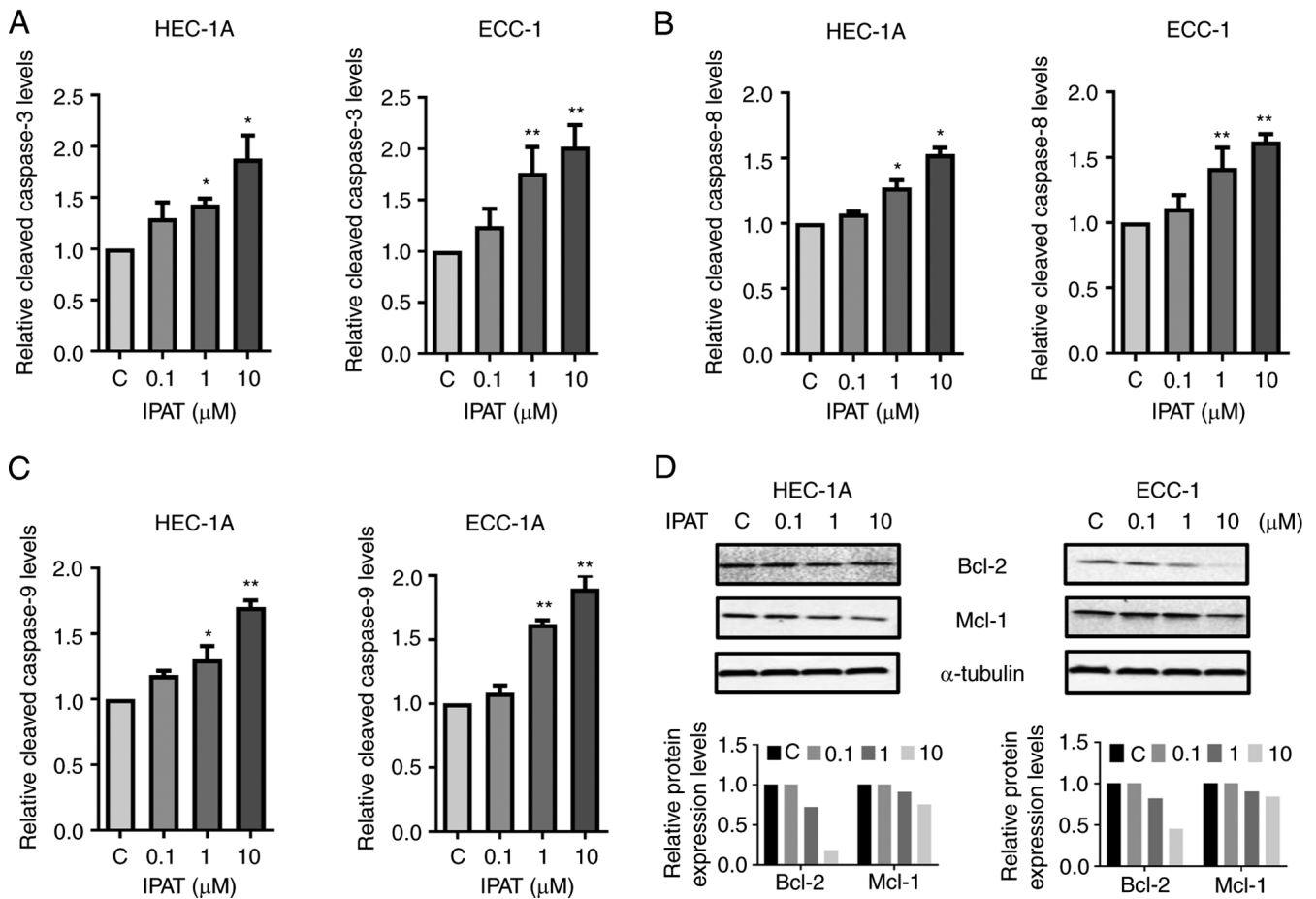


Figure 3. IPAT induced apoptosis in endometrial cancer cells. Cells were treated with the indicated concentrations of IPAT for 18 h. ELISA assays were used to assess the activities of (A) cleaved caspase 3, (B) 8 and (C) 9 in whole cell extracts. IPAT induced activities of cleaved caspase 3, 8 and 9 in a dose-dependent manner in both cell lines. (D) The protein expression levels of Bcl-2 and MCL-1 was assessed by western blotting. IPAT reduced the protein expression levels of Bcl-2 and MCL-1 in both cell lines * $P < 0.05$ and ** $P < 0.01$. IPAT, ipatasertib; C, control.

group (Fig. 6B). Furthermore, EC tissues from each treatment group and the control group were stained for the DNA damage marker p-H2AX and the microtubule motor protein KIF-14. The protein expression levels of p-H2AX and KIF14 in PTX and PTX + IPAT groups were significantly higher compared with those in the control and IPAT groups. Compared with the other groups, the combination of IPAT and PTX had the greatest effect on the protein expression levels of Ki67, p-S6, p-H2AX and KIF-14. These results suggested that IPAT increased sensitivity to PTX through DNA damage pathways in EC *in vivo*.

Effect of IPAT and PTX on cell proliferation in primary cultures of human EC. Given that primary cell cultures from human tumors have the potential capacity to predict the sensitivity of cytotoxic agents, which established cancer cell lines are not able to do (26), the effect of IPAT on cell proliferation was evaluated in primary cell cultures of human EC. A total of fourteen primary cell cultures of EC were isolated and cultured for the present study (Table I). Each cell culture was treated with different concentrations of IPAT, PTX and the combination for 24 and 72 h. Treatment with IPAT for 72 h resulted in reduced cell viability in 11/14 primary cultures, while all primary cultures exhibited diverse responses to PTX (Fig. 7A). The combination of low doses of IPAT and

PTX demonstrated synergistic responses in 8/14 primary cultured cells. The representative EC6 sample, demonstrated that the combined treatment increased inhibition of cell proliferation compared with PTX or IPAT alone (Fig. 7B). Three unresponsive IPAT primary cultures (EC9, EC11 and EC12) did not demonstrate any synergistic inhibition of cell proliferation in combination with PTX. Four of the 11 primary cultures which demonstrated an inhibitory response to IPAT were assayed for cleaved caspase 3 activity. The results demonstrated that the combination treatment had a markedly greater effect on inducing the activity of cleaved caspase 3 in three cases. The combined treatment increased the activity of cleaved caspase 3 in the representative EC6 sample, (Fig. 7C).

To evaluate the relationship between the expression of p-AKT and p-S6, and sensitivity to IPAT, the protein expression levels of p-AKT and S6 were assessed using western blotting in the 14 untreated primary cell cultures, HEC-1A and ECC-1 cells. Marked differential expression of p-AKT and p-S6 were demonstrated in primary cultures and EC cells (Fig. 7D). Sensitivity to IPAT was not associated with the protein expression levels of p-AKT or p-S6 through comparison of expression levels and sensitivity to IPAT using linear regression models in primary cultures and EC cell lines (Fig. 7E).

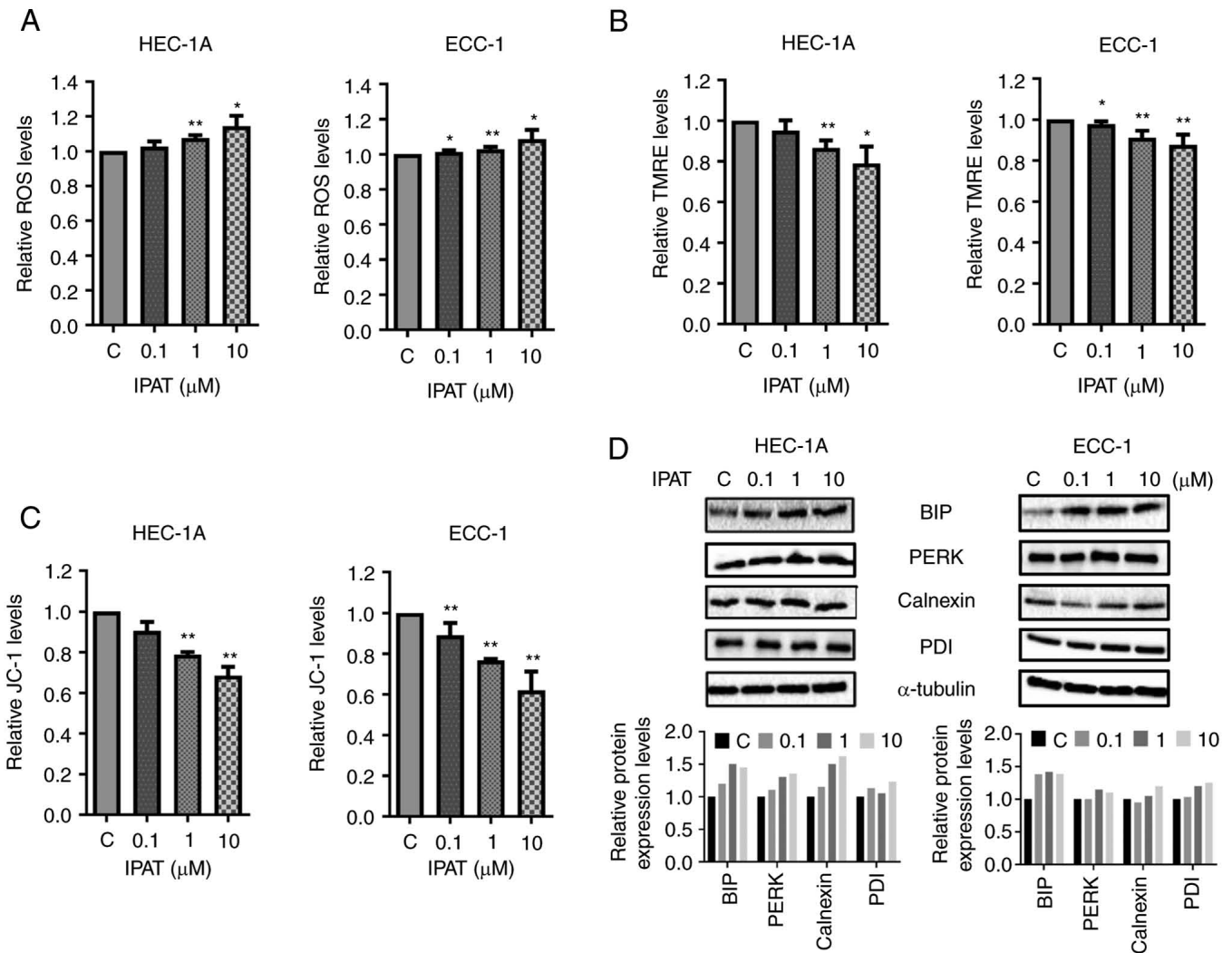


Figure 4. IPAT induced cellular stress in EC cells. Effects of IPAT on cellular stress and mitochondrial membrane potential in HEC-1A and ECC-1 cells were detected by the ROS, JC-1 and TMRE assays. HEC-1A and ECC-1 cell lines were treated with a range of concentrations of IPAT for 16 h, and (A) IPAT significantly increased the levels of intracellular ROS in a dose-dependent manner in both cell lines. (B) TMRE and (C) JC-1 assays demonstrated that IPAT decreased mitochondrial membrane potential in the HEC-1A and ECC-1 cells treated with IPAT for 16 h. (D) The protein expression levels of BIP, PERK, Calnexin and PDI was semi-quantified using western blotting which demonstrated that IPAT increased the protein expression levels of these proteins in both cell lines after 24 h of treatment. *P<0.05 and **P<0.01. IPAT, ipatasertib; C, control; ROS, reactive oxygen species; EC, endometrial cancer; TMRE, tetramethylrhodamine ethyl ester.

Discussion

More than 80% of patients with EC have ≥1 genetic alterations that affect the activity and function of the PI3K/AKT/mTOR signaling pathway and these alterations result in this pathway being the most commonly dysregulated signaling pathway in EC (27,28). IPAT is an orally administered direct inhibitor of all three isoforms of p-AKT that has been reported to have anti-tumor efficacy in numerous pre-clinical models (9-12). Recent phase I-II clinical trials have reported that oral daily IPAT was well tolerated with few adverse events and resulted in clinical activity (target engagement with a tolerable safety profile and limited cancer control) in advanced solid tumors (12,16,17). To generate pre-clinical data on the effect of IPAT on EC, the anti-proliferative and anti-tumorigenic effects of IPAT were assessed in human EC cell lines, primary cultures of EC and a transgenic mouse model of EC. Treating EC cell lines with IPAT led to marked inhibition of the AKT/mTOR

signaling pathway, markedly reduced cellular proliferation, and induced cellular stress, cell cycle G1 arrest and apoptosis. The combination of IPAT and PTX synergistically inhibited cell viability and induced apoptosis in EC cells and primary cultures of EC tumors, compared with treatment with either drug alone. Additionally, IPAT significantly reduced tumor growth and increased sensitivity to PTX in the *Lkb1^{fl/fl}p53^{fl/fl}* mouse model of EC, accompanied by a marked decrease in Ki67 and p-S6 protein expression levels and a marked increase in the protein expression levels of p-H2AX and KIF14 in endometrial tumor tissues. These data suggested that the targeting of AKT by IPAT not only effectively inhibited cell proliferation and tumor growth and but also enhanced the efficacy of PTX in the treatment of EC *in vitro* and *in vivo*.

Previous studies reported that IPAT increased the phosphorylation of AKT and decreased the phosphorylation of the proline rich AKT substrate PRAS40 in a dose dependent manner in cancer cells (18,29). Treatment with effective doses

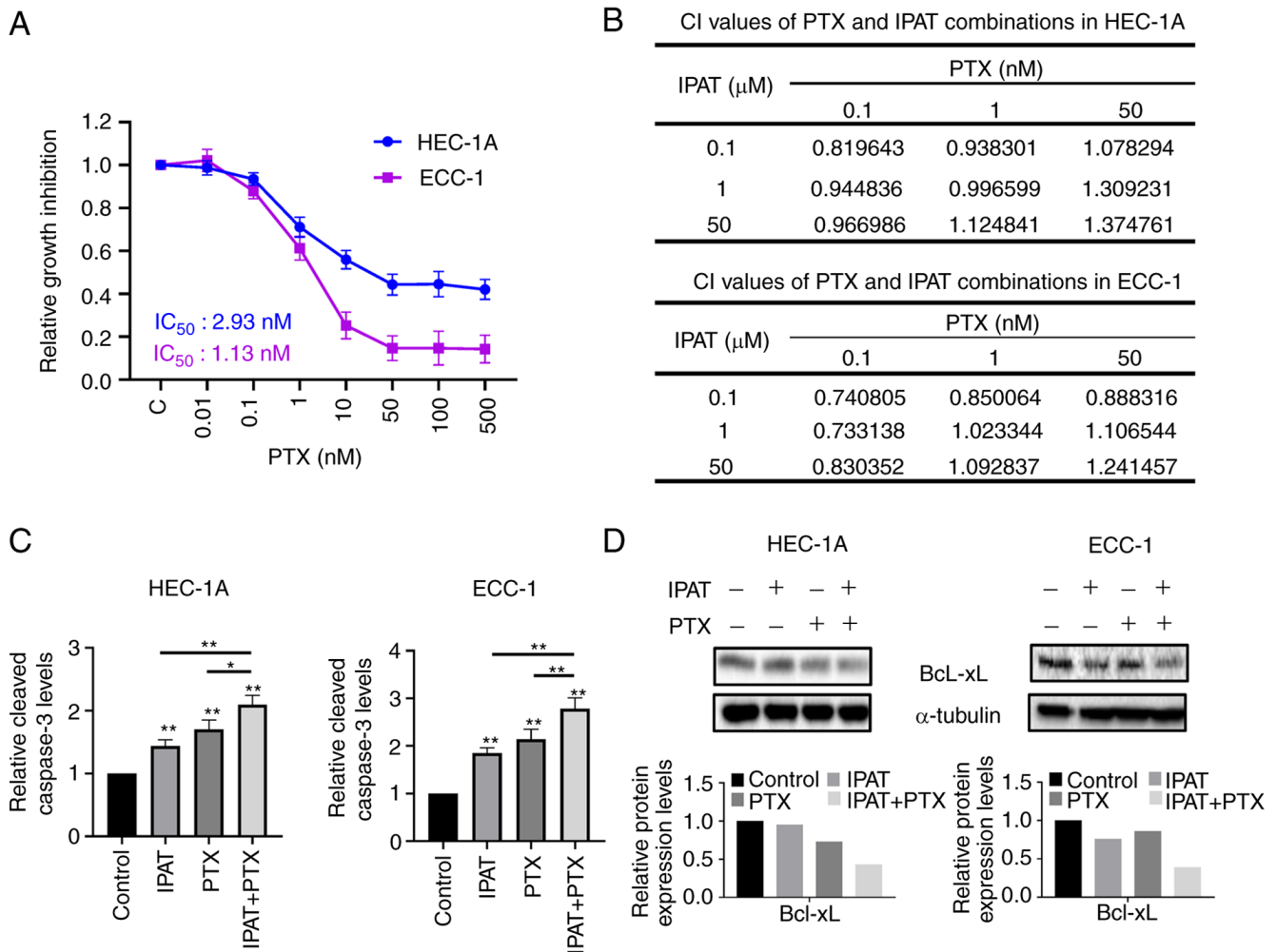


Figure 5. IPAT increased the sensitivity to PTX in EC cells. Both cell lines were treated with different concentrations of IPAT and PTX for 72 h. (A) An MTT assay demonstrated that PTX significantly reduced cell proliferation in a dose-dependent manner. (B) HEC-1A and ECC-1 were treated with the indicated concentrations of IPAT, PTX and the combination of IPAT + PTX for 72 h. Cell viability was determined by MTT assay. The CI was calculated by Bliss analysis. (C) Combination treatment demonstrated increased effects on cleaved caspase 3 activity compared with IPAT or PTX alone. (D) Western blotting analysis demonstrated that the combination treatment produced a more effective inhibitory effect on the expression of Bcl-xL in both cell lines after 24 h of treatment. * $P < 0.05$ and ** $P < 0.01$. IPAT, ipatasertib; PTX, paclitaxel; C, control; CI, combination index.

of IPAT with xenograft mouse cancer models can inhibit p-PRAS40 activity and target p-S6 in tumor tissue, which suggested that IPAT is a potent inhibitor of AKT/mTOR signaling and that inhibition of AKT/mTOR signaling is essential for a robust anticancer response *in vivo* (18,29). The results of our previous study demonstrated that IPAT increased phosphorylation of AKT (ser473) and decreased phosphorylation of S6 (ser235/236) in a dose- and time-dependent manner in USC cells, which provided further evidence that IPAT inhibits the AKT/mTOR pathway (19). Growing evidence has suggested that the activation of AKT/mTOR and its downstream signaling pathways is responsible for cell survival, angiogenesis, cell cycle progression, apoptosis and cellular stress, and subsequently, inhibition of the AKT/mTOR pathway results in inhibition of cell proliferation, cell cycle arrest, and the induction of apoptosis and cellular stress in EC cells (28,30). Previous studies of IPAT in numerous tumor types reported that IPAT inhibited the activity of the AKT/mTOR signaling pathway, induced cell cycle G1 arrest and increased apoptosis in cancer cells, which ultimately

resulted in a robust anti-tumorigenic response in xenograft models with a hyperactive PI3K/AKT/mTOR signaling pathway (18,31). Previous studies reported that IPAT inhibited tumor cell growth through numerous mechanisms, including activation of PUMA, FoxO3a and NF- κ B regulated apoptosis, as well as induction of autophagy signaling and ROS-mediated caspase activation (32-34). Importantly, compared with other allosteric AKT inhibitors such as MK-2206, IPAT was able to overcome MK-2206 resistance in prostate cancer cells and xenograft mouse models, thereby expanding the practicability of IPAT for clinical applications (35).

In the present study, similar effects of IPAT on phosphorylation of AKT (ser473) and S6 (ser235/236) were demonstrated in EC cells, which provided further evidence that IPAT is a potent inhibitor of the AKT/mTOR signaling pathway in EC. Treatment of EC cell lines with different concentrations of IPAT also reduced cell proliferation, caused cell cycle G1 phase arrest and induced mitochondrial apoptosis in a dose-dependent manner. Furthermore, IPAT was effective in inhibiting cell proliferation in 11/14 primary cultures and

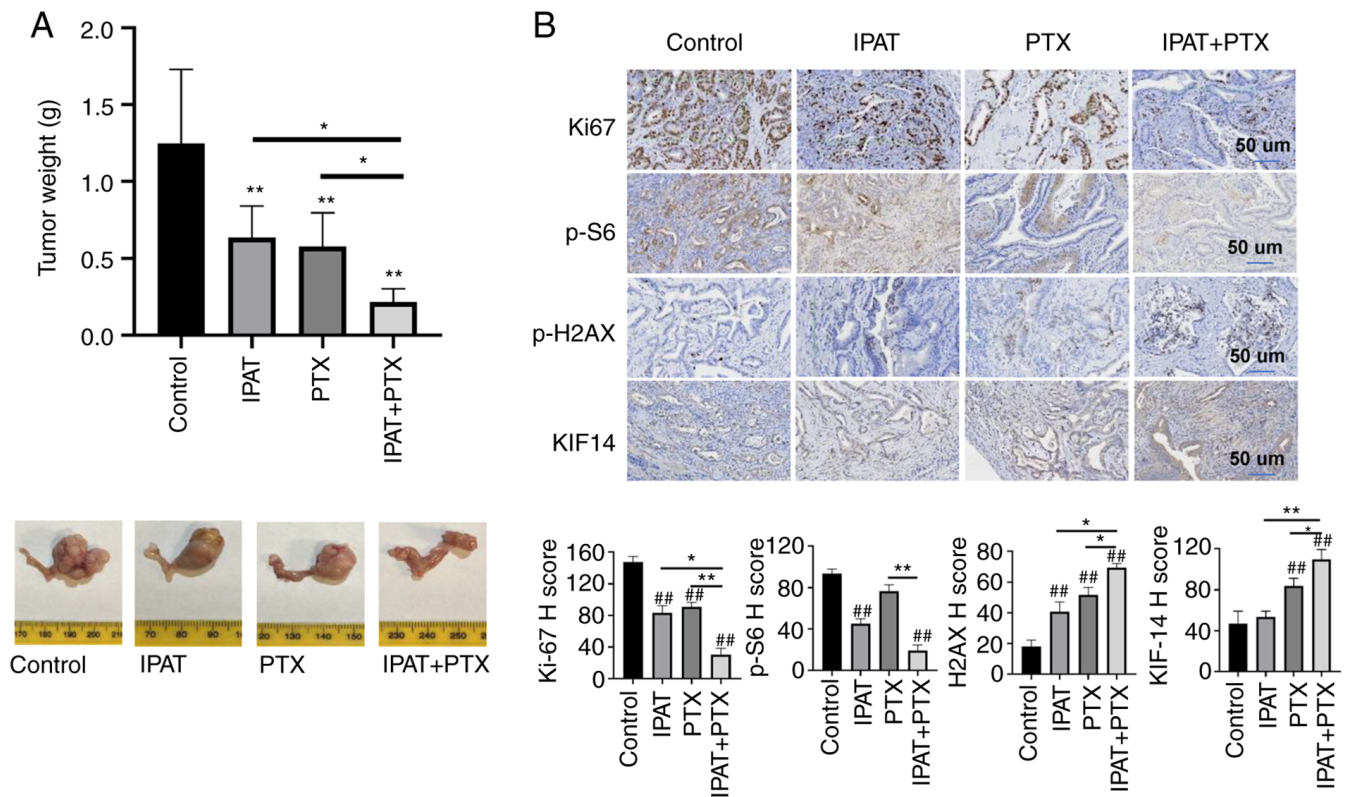


Figure 6. Effect of IPAT and PTX on tumor growth in *Lkb1^{fl/fl}p53^{fl/fl}* mice. *Lkb1^{fl/fl}p53^{fl/fl}* mice were divided into four groups: control, IPAT, PTX and IPAT + PTX. The mice were treated with IPAT (50 mg/kg, oral gavage, daily), PTX (10 mg/kg, intraperitoneal, weekly), the combination and vehicle for 4 weeks. (A) Average tumor weights from each group at the end of treatment were compared and analyzed. IPAT or PTX significantly inhibited tumor growth, and the combination treatment synergistically further inhibited tumor growth in the mice. (B) The expression of Ki67, p-S6, p-H2AX and KIF14 was assessed using immunohistochemical staining in the EC tissues. IHC results were scored by multiplying the percentage of positive cells (P) by the intensity (I). * $P < 0.05$ and ** $P < 0.01$. ## $P < 0.01$ vs. control. IPAT, ipatasertib; PTX, paclitaxel.

decreasing tumor growth with reduced protein expression levels of Ki67 and p-S6 in the *Lkb1^{fl/fl}p53^{fl/fl}* mouse model of EC. Taken together, these findings demonstrated the inhibitory effect of IPAT on the AKT/mTOR signaling pathway, and that the targeting of AKT by IPAT enables concomitant downregulation of p-S6 and suppresses tumor growth through a combination of increased cellular stress and induction of apoptosis and cell cycle arrest in EC.

Aberrant PI3K/AKT signaling regulates ROS production in cancer cells through multiple molecular mechanisms that contribute to the regulation of mitochondrial oxidative metabolism and NADPH oxidase activation (36). Elevated cellular ROS levels contribute to the loss of mitochondrial membrane potential and subsequently directly cause DNA damage, activate apoptotic and autophagy pathways, ultimately resulting in increased efficacy of anti-tumor agents or the reversal of chemotherapeutic resistance in cancer cells (37,38). IPAT significantly increased intracellular ROS level and activated apoptotic signaling pathways in TRAIL-resistant HT-29 cells, with reversal of TRAIL-resistance being dependent on ROS generation, DNA damage and p53-mediated PUMA up-regulation (32). The results of the present study support the role of IPAT in inducing ROS production as we found that IPAT decreased mitochondrial membrane potential in a dose-dependent manner in EC cells, which indicated that induction of ROS may be a critical early step in the anti-tumorigenic activity of IPAT. Due to the role of cellular stress in IPAT-induced growth

inhibition, further investigation of how IPAT-induced cellular stress affects apoptosis and cell growth inhibition in EC cells and *Lkb1^{fl/fl}p53^{fl/fl}* mouse model is required.

The PI3K/AKT signaling pathway participates in the regulation of oncogenic activity and the development of resistance in cancer cells to various chemotherapeutic drugs. Each AKT isoform exhibits different biologic functions and has a distinct impact on chemoresistance to chemotherapeutic agents including PTX, cisplatin and doxorubicin in EC cell lines (39,40). AKT inhibition enhances the effect of cytotoxic agents, and the AKT inhibitor AZD5363, in combination with chemotherapeutic drugs, markedly reduces cell viability and induces apoptosis in EC cells (41). Alteration of AKT activity induced by chemotherapeutic agents may be an intrinsic or adaptive resistance mechanism for cancer survival; therefore, targeting AKT might be used to improve sensitivity to chemotherapeutic agents and promote therapeutic efficacy (12). Two randomized phase II clinical trials have reported that the combination of IPAT with PTX was well tolerated and significantly improved PFS compared with PTX alone in inoperable locally advanced/metastatic triple-negative breast cancer (13,20). Although a recent phase III clinical trial reported no improvement in efficacy for IPAT + PTX in PIK3CA/AKT1/PTEN-altered hormone receptor-positive HER2-negative advanced breast cancer, the safety profile for the combination treatment was consistent with known adverse effects of IPAT alone and PTX alone (42). Although PTX has

Table I. Clinical and pathological characteristics of 14 patients with endometrial carcinoma.

Case	Age	Race	Figo stage ^a	Tumor size, cm	Histology	HER2
EC1	54	Hispanic (White)	IA	3.5	Endometrioid, grade 2	Negative
EC2	73	White	IA	4.5	Endometrioid, grade 1	Negative
EC3	46	Hispanic (White)	IA	2.2	Endometrioid, grade 1	N/A
EC4	46	Black	IA	3.5	Endometrioid, grade 3	N/A
EC5	63	Black	IA	4.5	Endometrioid, grade 1	N/A
EC6	43	Black	IIIC1	0.5	Endometrioid, grade 1	N/A
EC7	80	White	IB	5.3	Endometrioid, grade 2	N/A
EC8	40	White	IA	3.7	Endometrioid, grade 1	N/A
EC9	67	White	IA	4.8	Endometrioid, grade 2	N/A
EC10	74	White	IB	6	Endometrioid, grade 1	N/A
EC11	54	Hispanic (White)	IA	3.3	Endometrioid, grade 1	N/A
EC12	64	White	IB	5	Dedifferentiated endometrial adenocarcinoma	N/A
EC13	69	White	IA	3.3	Endometrioid, grade 1	N/A
EC14	73	White	IA	2.6	Uterine carcinosarcoma	N/A

^aFIGO 2009 (47). EC, endometrial cancer; N/A, not tested.

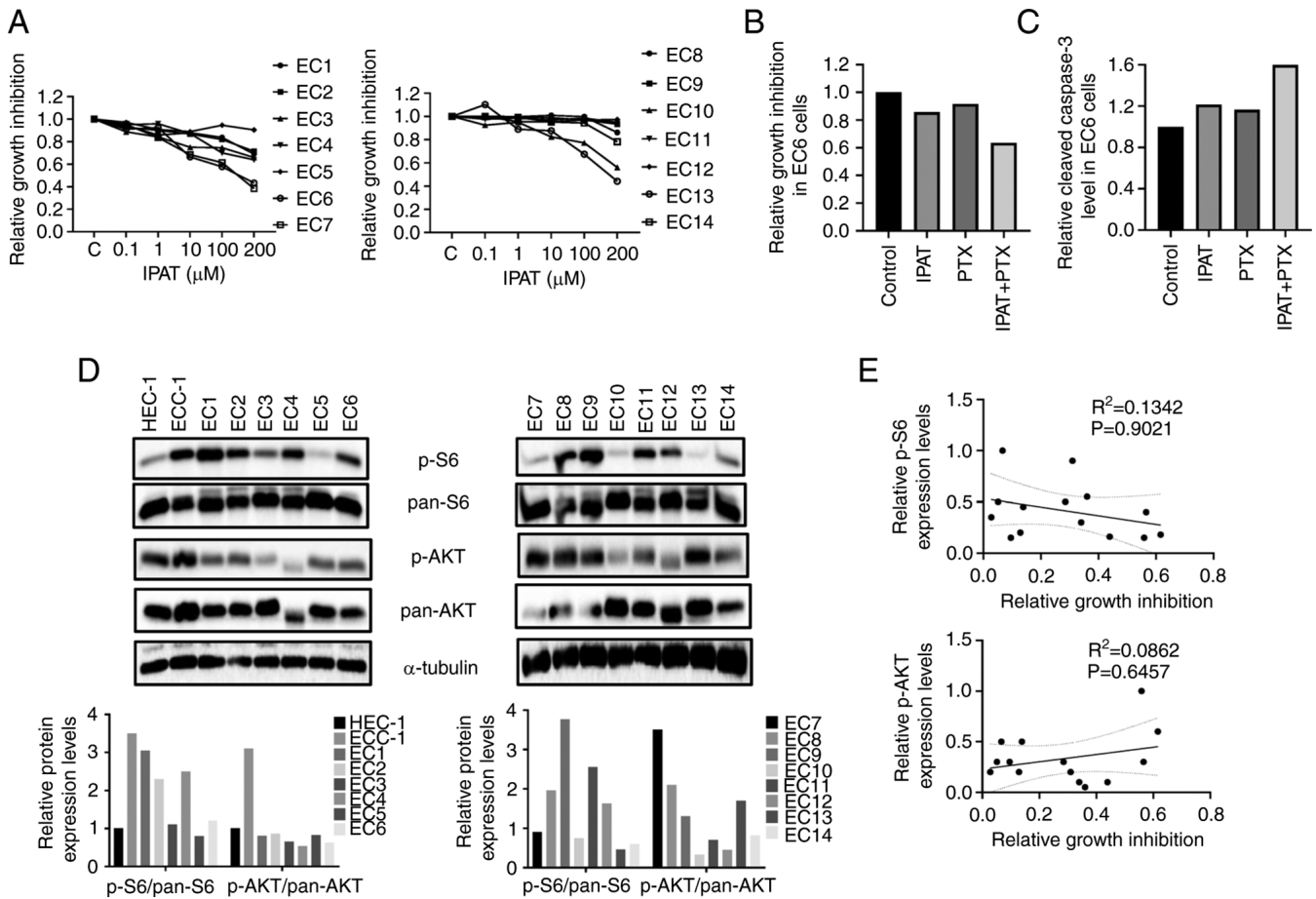


Figure 7. Effect of IPAT on cell viability in primary cultures of EC. Fourteen human EC tissues were collected, and primary epithelial tumor cells were isolated. The cells were plated into 96 well plates and treated with IPAT for 72 h. (A) An MTT assay indicated that IPAT exhibited inhibitory effects on cell proliferation in 11/14 primary cell cultures of EC. The primary cultures of EC6 cells were treated with 1 μ M IPAT, 1 nM PTX or combination for 72 h for MTT assay, or for 18 h for measurement of cleaved caspase 3 activity. The results demonstrated that the combination treatment produced greater effects on (B) cell proliferation and (C) cleaved caspase 3 activity in the primary cultures of EC6 cells. (D) The protein expression levels of p-AKT and p-S6 was semi-quantified using western blotting in the HEC-1A, ECC-1 and 14 primary culture cells. (E) The phosphorylation of AKT (ser473) and S6 (ser235/236) was not associated with the sensitivity of IPAT in EC cell lines or primary cultures of EC. IPAT, ipatasertib; PTX, paclitaxel; p, phosphorylated; EC, endometrial cancer.

been reported to display its anticancer effects by promoting microtubule polymerization and stabilization and arresting cells in the metaphase of the bipolar spindle, its ability to cause DNA damage and induce oxidative stress and apoptosis which suggested that PTX may have other cellular cytotoxic modes of action (43,44). In the present study, the possible synergistic effect of the combination of IPAT and PTX was evaluated and it was demonstrated that the combination of IPAT and PTX significantly enhanced the cytotoxic and apoptotic properties of either drug alone in EC cells or primary cultures of EC. Furthermore, IPAT + PTX demonstrated potent inhibition of tumor growth with increased expression of DNA damage and microtubule markers and markedly decreased the expression of p-S6, compared with IPAT alone or PTX alone in the *Lkb1^{fl/fl}p53^{fl/fl}* mouse model, which indicated that IPAT may potentiate the efficacy of PTX. Thus, it was hypothesized that increased DNA damage, inhibited AKT/mTOR/S6 pathway and altered microtubule function; moreover, altered microtubule function may be potential mechanisms by which the combination of IPAT and PTX synergistically inhibits EC tumor growth.

Inhibition of p-AKT enhances the effect of cytotoxic agents, which indicated that p-AKT levels could be associated with sensitivity to cytotoxic agents (12,45). High expression of p-AKT strongly predicted the sensitivity to IPAT in multiple pre-clinical cancer models (18,31). In the double-blind randomized phase II FAIRLANE trial, cancer patients with high p-AKT scores, but not mTOR scores, demonstrated significantly higher objective response rates with IPAT treatment, which indicated that baseline functional protein levels of p-AKT might have predictive value for IPAT (46). However, our previous study demonstrated that baseline expression of p-AKT and S6 was independent of cell sensitivity to inhibition by IPAT in primary cultures of USC and USC cell lines (19). Similar results were demonstrated in the present study. By analyzing the baseline protein expression levels of p-AKT and S6 and the sensitivity of IPAT to inhibit cell growth, it was demonstrated that the expression levels of p-AKT and p-S6 in EC cell lines and primary cultures were not correlated with the sensitivity of IPAT to inhibit cell proliferation. Due to its potential clinical importance, further work will be needed to identify the relationship between IPAT sensitivity and the expression of p-AKT and S6 in future EC clinical trials.

In summary, the present study evaluated the potential effects of IPAT and the combination of IPAT + PTX on cell proliferation and tumor growth in human endometrioid EC cells, primary cultures of endometrioid EC tumors and the *Lkb1^{fl/fl}p53^{fl/fl}* mouse model of endometrioid EC. Our results demonstrated that IPAT inhibited cell viability and tumor growth through the induction of cellular stress, cell cycle G1 arrest and apoptosis, and that IPAT synergistically potentiated the effect of PTX on tumor growth inhibition. These results provided a strong biological rationale for clinical trials investigating IPAT alone and the combination of IPAT and PTX in patients with EC.

Acknowledgements

Not applicable.

Funding

This work was supported by The Endometrial Cancer Molecularly Targeted Therapy Consortium and The National Institutes of Health/National Cancer Institute (grant no. R37CA226969).

Availability of data and materials

The datasets used and/or analyzed during the current study are available from the corresponding author on reasonable request.

Authors' contributions

JO, ZZ, LB, TH, XZ, YF, HS and WS performed the experiments. JO, ZZ, TH, CJ, BD, XS and CZ analyzed and interpreted the data. JO, ZZ, and CZ wrote the manuscript. AAS, CZ and VB designed experiments, revised the manuscript and obtained funding. All authors read and approved the final manuscript.

Ethics approval and consent to participate

All patients provided written informed consent and were approved by the Institutional Review Board of the University of North Carolina at Chapel Hill (approval no. 20-3013). Animal study was approved by the UNC-CH Institutional Animal Care and Use Committee (approval no. 20-219).

Patient consent for publication

Not applicable.

Competing interests

The authors declare that they have no competing interests.

References

1. Siegel RL, Miller KD, Wagle NS and Jemal A: Cancer statistics, 2023. *CA Cancer J Clin* 73: 17-48, 2023.
2. Crosbie EJ, Kitson SJ, McAlpine JN, Mukhopadhyay A, Powell ME and Singh N: Endometrial cancer. *Lancet* 399: 1412-1428, 2022.
3. Tronconi F, Nero C, Giudice E, Salutari V, Musacchio L, Ricci C, Carbone MV, Ghizzoni V, Perri MT, Camarda F, *et al.*: Advanced and recurrent endometrial cancer: State of the art and future perspectives. *Crit Rev Oncol Hematol* 180: 17, 2022.
4. Makker V, Green AK, Wenham RM, Mutch D, Davidson B and Miller DS: New therapies for advanced, recurrent, and metastatic endometrial cancers. *Gynecol Oncol Res Pract* 4: 19, 2017.
5. Nero C, Tronconi F, Giudice E, Scambia G and Lorusso D: Management of stage III and IVa uterine cancer. *Int J Gynecol Cancer* 32: 316-322, 2022.
6. van den Heerik A, Horeweg N, de Boer SM, Bosse T and Creutzberg CL: Adjuvant therapy for endometrial cancer in the era of molecular classification: Radiotherapy, chemoradiation and novel targets for therapy. *Int J Gynecol Cancer* 31: 594-604, 2021.
7. LoRusso PM: Inhibition of the PI3K/AKT/mTOR pathway in solid tumors. *J Clin Oncol* 34: 3803-3815, 2016.
8. Roncolato F, Lindemann K, Willson ML, Martyn J and Mileschkin L. PI3K/AKT/mTOR inhibitors for advanced or recurrent endometrial cancer. *Cochrane Database Syst Rev* 10: CD012160, 2019.

9. Bang YJ, Kang YK, Ng M, Chung HC, Wainberg ZA, Gendreau S, Chan WY, Xu N, Maslyar D, Meng R, *et al*: A phase II, randomised study of mFOLFOX6 with or without the Akt inhibitor ipatasertib in patients with locally advanced or metastatic gastric or gastroesophageal junction cancer. *Eur J Cancer* 108: 17-24, 2019.
10. Chan JJ, Tan TJY and Dent RA: Novel therapeutic avenues in triple-negative breast cancer: PI3K/AKT inhibition, androgen receptor blockade, and beyond. *Ther Adv Med Oncol* 11: 1758835919880429, 2019.
11. de Bono JS, De Giorgi U, Rodrigues DN, Massard C, Bracarda S, Font A, Arranz Arija JA, Shih KC, Radavoi GD, Xu N, *et al*: Randomized phase II study evaluating akt blockade with ipatasertib, in combination with abiraterone, in patients with metastatic prostate cancer with and without PTEN loss. *Clin Cancer Res* 25: 928-936, 2019.
12. Isakoff SJ, Taberero J, Molife LR, Soria JC, Cervantes A, Vogelzang NJ, Patel MR, Hussain M, Baron A, Argilés G, *et al*: Antitumor activity of ipatasertib combined with chemotherapy: Results from a phase Ib study in solid tumors. *Ann Oncol* 31: 626-633, 2020.
13. Kim SB, Dent R, Im SA, Espié M, Blau S, Tan AR, Isakoff SJ, Oliveira M, Saura C, Wongchenko MJ, *et al*: Ipatasertib plus paclitaxel versus placebo plus paclitaxel as first-line therapy for metastatic triple-negative breast cancer (LOTUS): A multicentre, randomised, double-blind, placebo-controlled, phase 2 trial. *Lancet Oncol* 18: 1360-1372, 2017.
14. Morgillo F, Della Corte CM, Diana A, Mauro CD, Ciaramella V, Barra G, Belli V, Franzese E, Bianco R, Maiello E, *et al*: Phosphatidylinositol 3-kinase (PI3K α)/AKT axis blockade with taselisib or ipatasertib enhances the efficacy of anti-microtubule drugs in human breast cancer cells. *Oncotarget* 8: 76479-76491, 2017.
15. Oliveira M, Saura C, Nuciforo P, Calvo I, Andersen J, Passos-Coelho JL, Gil Gil M, Bermejo B, Patt DA, Ciruelos E, *et al*: FAIRLANE, a double-blind placebo-controlled randomized phase II trial of neoadjuvant ipatasertib plus paclitaxel for early triple-negative breast cancer. *Ann Oncol* 30: 1289-1297, 2019.
16. Saura C, Roda D, Roselló S, Oliveira M, Macarulla T, Pérez-Fidalgo JA, Morales-Barrera R, Sanchis-García JM, Musib L, Budha N, *et al*: A First-in-Human phase I study of the ATP-competitive AKT inhibitor ipatasertib demonstrates robust and safe targeting of AKT in patients with Solid tumors. *Cancer Discov* 7: 102-113, 2017.
17. Shapiro GI, LoRusso P, Cho DC, Musib L, Yan Y, Wongchenko M, Chang I, Patel P, Chan IT, Sanabria-Bohorquez S, *et al*: A phase Ib open-label dose escalation study of the safety, pharmacokinetics, and pharmacodynamics of cobimetinib (GDC-0973) and ipatasertib (GDC-0068) in patients with locally advanced or metastatic solid tumors. *Invest New Drugs* 39: 163-174, 2021.
18. Lin J, Sampath D, Nannini MA, Lee BB, Degtyarev M, Oeh J, Savage H, Guan Z, Hong R, Kassees R, *et al*: Targeting activated Akt with GDC-0068, a novel selective Akt inhibitor that is efficacious in multiple tumor models. *Clin Cancer Res* 19: 1760-1772, 2013.
19. Buckingham L, Hao T, O'Donnell J, Zhao Z, Zhang X, Fan Y, Sun W, Zhang Y, Suo H, Secord AA, *et al*: Ipatasertib, an oral AKT inhibitor, inhibits cell proliferation and migration, and induces apoptosis in serous endometrial cancer. *Am J Cancer Res* 12: 2850-2862, 2022.
20. Dent R, Oliveira M, Isakoff SJ, Im SA, Espié M, Blau S, Tan AR, Saura C, Wongchenko MJ, Xu N, *et al*: Final results of the double-blind placebo-controlled randomized phase 2 LOTUS trial of first-line ipatasertib plus paclitaxel for inoperable locally advanced/metastatic triple-negative breast cancer. *Breast Cancer Res Treat* 189: 377-386, 2021.
21. Sweeney C, Bracarda S, Sternberg CN, Chi KN, Olmos D, Sandhu S, Massard C, Matsubara N, Alekseev B, Parnis F, *et al*: Ipatasertib plus abiraterone and prednisolone in metastatic castration-resistant prostate cancer (IPATentia150): A multicentre, randomised, double-blind, phase 3 trial. *Lancet* 398: 131-142, 2021.
22. Guo H, Kong W, Zhang L, Han J, Clark LH, Yin Y, Fang Z, Sun W, Wang J, Gilliam TP, *et al*: Reversal of obesity-driven aggressiveness of endometrial cancer by metformin. *Am J Cancer Res* 9: 2170-2193, 2019.
23. Staley A, Tucker K, Yin Y, Zhang X, Fan Y, Zhang Y, Fang Z, Sun W, Suo H, Zhao X, *et al*: Highly potent dopamine receptor D2 antagonist ONC206 demonstrates anti-tumorigenic activity in endometrial cancer. *Am J Cancer Res* 11: 5374-5387, 2021.
24. Pierce SR, Fang Z, Yin Y, West L, Asher M, Hao T, Zhang X, Tucker K, Staley A, Fan Y, *et al*: Targeting dopamine receptor D2 as a novel therapeutic strategy in endometrial cancer. *J Exp Clin Cancer Res* 40: 61, 2021.
25. Kaminskyy VO and Zhivotovsky B: Free radicals in cross talk between autophagy and apoptosis. *Antioxid Redox Signal* 21: 86-102, 2014.
26. Kodack DP, Farago AF, Dastur A, Held MA, Dardaei L, Friboulet L, von Flotow F, Damon LJ, Lee D, Parks M, *et al*: Primary patient-derived cancer cells and their potential for personalized cancer patient care. *Cell Rep* 21: 3298-3309, 2017.
27. Cheung LW, Hennessy BT, Li J, Yu S, Myers AP, Djordjevic B, Lu Y, Stenke-Hale K, Dyer MD, Zhang F, *et al*: High frequency of PIK3R1 and PIK3R2 mutations in endometrial cancer elucidates a novel mechanism for regulation of PTEN protein stability. *Cancer Discov* 1: 170-185, 2011.
28. Mazloumi Gavgani F, Smith Arnesen V, Jacobsen RG, Krakstad C, Hoivik EA and Lewis AE: Class I Phosphoinositide 3-Kinase PIK3CA/p110 α and PIK3CB/p110 β Isoforms in Endometrial Cancer. *Int J Mol Sci* 19: 3931, 2018.
29. Lin K, Lin J, Wu WI, Ballard J, Lee BB, Gloor SL, Vigers GP, Morales TH, Friedman LS, Skelton N and Brandhuber BJ: An ATP-site on-off switch that restricts phosphatase accessibility of Akt. *Sci Signal* 5: ra37, 2012.
30. Pavlidou A and Vlahos NF: Molecular alterations of PI3K/Akt/mTOR pathway: A therapeutic target in endometrial cancer. *ScientificWorldJournal* 2014: 709736, 2014.
31. Blake JF, Xu R, Bencsik JR, Xiao D, Kallan NC, Schlachter S, Mitchell IS, Spencer KL, Banka AL, Wallace EM, *et al*: Discovery and preclinical pharmacology of a selective ATP-competitive Akt inhibitor (GDC-0068) for the treatment of human tumors. *J Med Chem* 55: 8110-8127, 2012.
32. Yu L, Liu Z, Qiu L, Hao L and Guo J: Ipatasertib sensitizes colon cancer cells to TRAIL-induced apoptosis through ROS-mediated caspase activation. *Biochem Biophys Res Commun* 519: 812-818, 2019.
33. Cocco S, Leone A, Roca MS, Lombardi R, Piezzo M, Caputo R, Ciardiello C, Costantini S, Bruzzese F, Sisalli MJ, *et al*: Inhibition of autophagy by chloroquine prevents resistance to PI3K/AKT inhibitors and potentiates their antitumor effect in combination with paclitaxel in triple negative breast cancer models. *J Transl Med* 20: 290, 2022.
34. Sun L, Huang Y, Liu Y, Zhao Y, He X, Zhang L, Wang F and Zhang Y: Ipatasertib, a novel Akt inhibitor, induces transcription factor FoxO3a and NF- κ B directly regulates PUMA-dependent apoptosis. *Cell Death Dis* 9: 911, 2018.
35. Savill KMZ, Lee BB, Oeh J, Lin J, Lin E, Chung WJ, Young A, Chen W, Miš M, Mesh K, *et al*: Distinct resistance mechanisms arise to allosteric vs. ATP-competitive AKT inhibitors. *Nat Commun* 13: 2057, 2022.
36. Koundourou N and Poulgiannis G: Phosphoinositide 3-Kinase/Akt signaling and redox metabolism in cancer. *Front Oncol* 8: 160, 2018.
37. Aggarwal V, Tuli HS, Varol A, Thakral F, Yerer MB, Sak K, Varol M, Jain A, Khan MA and Sethi G: Role of reactive oxygen species in cancer progression: Molecular mechanisms and recent advancements. *Biomolecules* 9: 735, 2019.
38. Asaduzzaman Khan M, Tania M, Zhang DZ and Chen HC: Antioxidant enzymes and cancer. *Chin J Cancer Res* 22: 87-92, 2010.
39. Girouard J, Lafleur MJ, Parent S, Leblanc V and Asselin E: Involvement of Akt isoforms in chemoresistance of endometrial carcinoma cells. *Gynecol Oncol* 128: 335-343, 2013.
40. Gagnon V, Van Themsche C, Turner S, Leblanc V and Asselin E: Akt and XIAP regulate the sensitivity of human uterine cancer cells to cisplatin, doxorubicin and taxol. *Apoptosis* 13: 259-271, 2008.
41. Fabi F, Adam P, Parent S, Tardif L, Cadrin M and Asselin E: Pharmacologic inhibition of Akt in combination with chemotherapeutic agents effectively induces apoptosis in ovarian and endometrial cancer cell lines. *Mol Oncol* 15: 2106-2119, 2021.
42. Turner N, Dent RA, O'Shaughnessy J, Kim SB, Isakoff SJ, Barrios C, Saji S, Bondarenko I, Nowecki Z, Lian Q, *et al*: Ipatasertib plus paclitaxel for PIK3CA/AKT1/PTEN-altered hormone receptor-positive HER2-negative advanced breast cancer: Primary results from cohort B of the IPATunity130 randomized phase 3 trial. *Breast Cancer Res Treat* 191: 565-576, 2022.
43. Veerabhadrapa B, Subramanian S, S J S and Dyavaiah M: Evaluating the genetic basis of anti-cancer property of Taxol in *Saccharomyces cerevisiae* model. *FEMS Microbiol Lett* 368: fnab077, 2021.

44. Zhao X, Kong W, Tucker K, Staley A, Fan Y, Sun W, Yin Y, Huang Y, Fang Z, Wang J, *et al*: SPR064, a pro-drug of paclitaxel, has anti-tumorigenic effects in endometrial cancer cell lines and mouse models. *Am J Transl Res* 12: 4264-4276, 2020.
45. Shariati M and Meric-Bernstam F: Targeting AKT for cancer therapy. *Expert Opin Investig Drugs* 28: 977-988, 2019.
46. Shi Z, Wulfkuhle J, Nowicka M, Gallagher RI, Saura C, Nuciforo PG, Calvo I, Andersen J, Passos-Coelho JL, Gil-Gil MJ, *et al*: Functional mapping of AKT signaling and biomarkers of response from the FAIRLANE trial of neoadjuvant ipatasertib plus paclitaxel for triple-negative breast cancer. *Clin Cancer Res* 28: 993-1003, 2022.
47. Kasius JC, Pijnenborg JMA, Lindemann K, Forsse D, van Zwol J, Kristensen GB, Krakstad C, Werner HMJ and Amant F: Risk stratification of endometrial cancer patients: FIGO stage, biomarkers and molecular classification. *Cancers* 13: 5848, 2021.



Copyright © 2023 O'Donnell et al. This work is licensed under a Creative Commons Attribution-NonCommercial-NoDerivatives 4.0 International (CC BY-NC-ND 4.0) License.